Supplementary Information:

Graph neural network with classifications accelerating the discovery of Heusler catalysts for nitrogen reduction reaction

Jing Zhou[1], Xiayong Chen[1], Xiao Jiang[2], Zean Tian[2], Wangyu Hu[1], Bowen Huang*[1], and Dingwang Yuan*[1]

1 College of Materials Science and Engineering, Hunan University, Changsha 410082, China

2 College of Computer Science and Electronic Engineering, Hunan University, Changsha 410082, China

Supplementary Table 1: Category, range, and unit for features in node (atom) and edge (bond) vectors, respectively.

Input features in node (atom) vectors	category	range	unit
radius	10	0.32 ~ 1.62	Å
weight	10	1.01 ~ 208.98	g/mol
volume	10	4.68 ~ 21.37	cm^3/mol
electronegativity	10	1.22 ~ 3.04	
affinity	10	-0.7 ~ 2.31	eV
ionization	10	5.79 ~ 14.53	eV
Zeff	10	1.0 ~ 4.94	
group	14	1 ~ 15	
period	6	1 ~ 6	
d-electron	11	0 ~ 10	
Input features in edge (bond) vectors	**category**	**range**	**unit**
bond type	3		
distance to adsorbate on adsorbate-site graph	3		
distance to adsorbate on slab graph	5		

Supplementary Table 2: Hyperparameters for training process and for each model. The two sets of hyperparameters in the CGCNN correspond to the CGCNN with low MAE and with high accuracy for classification.

Hyperparameters on training process	Range	Selected parameter
Weight coefficient of the loss function		0.662
Learning rate		0.01
Epoch		1000
Weight decay		0.001
Batch size		256
Hyperparameters on the ASGCNN	**Range**	**Selected parameter**
Number of convolutional layers	1, 2, 3, 4, 5	3
Number of nodes in adsorption site graph embedding layer	60, 70, …, 200	110
Number of nodes in slab graph embedding layer	60, 70, …, 200	150
Number of nodes in the first hidden layer	10, 20, …, 200	80
Number of nodes in the second hidden layer	10, 20, …, 160	120
Number of nodes in the third hidden layer	10, 20, …, 160	10
Hyperparameters on the CGCNN	**Range**	**Selected parameter**
Number of convolutional layers	1, 2, 3, 4, 5	3/3
Number of nodes in slab graph embedding layer	60, 70, …, 200	190/150
Number of nodes in the first hidden layer	10, 20, …, 160	170/80
Number of nodes in the second hidden layer	10, 20, …, 160	30/20
Number of nodes in the third hidden layer	10, 20, …, 160	60/10
Hyperparameters on the SGCNN	**Range**	**Selected parameter**
Number of convolutional layers	1, 2, 3, 4, 5	4
Number of nodes in slab and bulk graph embedding layers	60, 70, …, 200	90
Number of nodes in the first hidden layer	10, 20, …, 160	70
Number of nodes in the second hidden layer	10, 20, …, 160	10
Number of nodes in the third hidden layer	10, 20, …, 160	70

Supplementary Table 3: R^2 score, MAE, RMSE, site accuracy and adsorbate accuracy for each mode. All the training processes are carried out under the same random number.

Mode		R^2	MAE	RMSE	site accuracy	adsorbate accuracy
ASGCNN	train	1.000	0.018	0.023		
	valid	0.974	0.117	0.197		
	test	0.955	0.153	0.259		
origin SGCNN	train	0.967	0.163	0.219		
	valid	0.943	0.218	0.292		
	test	0.928	0.234	0.328		
SGCNN	train	0.999	0.027	0.035		
	valid	0.975	0.117	0.192		
	test	0.959	0.149	0.248		
CGCNN	train	0.868	0.033	0.439		
	valid	0.977	0.114	0.186		
	test	0.955	0.152	0.258		
ASGCNN with	train	1.000	0.018	0.023	0.637	0.753
fixed parameters	valid	0.974	0.117	0.197	0.636	0.758
	test	0.955	0.153	0.259	0.650	0.752
ASGCNN	train	1.000	0.006	0.008	1	1
	valid	0.975	0.113	0.195	1	1
	test	0.958	0.145	0.252	1	1
ASGCNN	train	1.000	0.013	0.017	1	1
+ snapshot	valid	0.977	0.105	0.185	1	1
	test	0.961	0.132	0.242	1	1
SGCNN	train	1.000	0.007	0.008	1	1
	valid	0.939	0.218	0.301	1	1
	test	0.934	0.220	0.314	1	1
CGCNN with	train	1.000	0.006	0.007	1	1
low MAE	valid	0.974	0.112	0.196	1	1
	test	0.955	0.146	0.261	0.998	1
CGCNN with	train	1.000	0.015	0.021	1	1
low MAE	valid	0.977	0.109	0.186	1	1
+ snapshot	test	0.956	0.144	0.258	1	1
CGCNN with	train	1.000	0.006	0.007	1	1
high accuracy	valid	0.970	0.116	0.195	1	1
	test	0.952	0.153	0.269	1	1

Supplementary Table 4: Candidates obtained by loosen criteria (Uncertainty is not considered, $|U_L(HER)| - |U_L(NRR)| > 0.1$ eV and $\Delta G_r(NH_3(g)) - \Delta G_r(*NH_2) < 0.9$ eV). All units are eV.

	system	$\Delta G_r(*N_2)$	$\Delta G_r(*N_2) - \Delta G_r(*H)$	$\Delta G_r(*NNH) - \Delta G_r(*H)$	PDS	barrier	$\lvert\Delta U_L(HER)\rvert - \lvert U_L(NRR)\rvert$	$\Delta G_r(NH_3(g)) - \Delta G_r(*NH_2)$
1	Co_2YAl	-1.22	-0.49	-0.03	NH-NH_2	0.47	0.26	0.67
2	Co_2ZrZn	-1.33	-0.61	-0.19	NH-NH_2	0.49	0.24	0.87
3	Ni_2YAl	-0.91	-0.32	-0.10	NH-NH_2	0.30	0.29	0.80
4	Ni_2YGa	-1.04	-0.48	-0.25	NH-NH_2	0.41	0.15	0.86
5	Ni_2YZn	-1.05	-0.40	-0.19	NH-NH_2	0.46	0.19	0.82
6	Os_2HfGa	-1.01	-0.27	-0.06	NH-NH_2	0.33	0.40	0.87
7	Os_2HfIn	-1.22	-0.63	-0.44	NH-NH_2	0.46	0.13	0.77
8	Os_2HfSn	-0.96	-0.35	-0.09	NH-NH_2	0.26	0.34	0.76
9	Os_2ScGe	-1.18	-0.42	-0.02	NH-NH_2	0.45	0.30	0.84
10	Os_2TiGa	-0.94	-0.29	-0.01	NH-NH_2	0.45	0.20	0.87
11	Os_2ZrGa	-1.00	-0.25	-0.06	NH-NH_2	0.39	0.36	0.89
12	Os_2ZrSn	-0.91	-0.28	-0.02	NH-NH_2	0.35	0.27	0.74
13	Pt_2TiB	-0.32	-0.90	-0.81	N_2-NNH	0.09	0.49	0.86
14	Pt_2TiGe	-0.28	-0.63	-0.54	NH-NH_2	0.16	0.19	0.79
15	Rh_2MoZn	-0.66	-0.28	-0.11	N_2-NNH	0.17	0.21	0.84
16	Rh_2NbIn	-0.55	-0.22	-0.03	N_2-NNH	0.19	0.14	0.84
17	Rh_2ZrB	-0.27	-0.64	-0.67	N_2-NNH	0.00	0.37	0.78
18	Ru_2HfB	-0.88	-0.47	-0.23	N_2-NNH	0.24	0.17	0.48
19	Ru_2HfGa	-1.01	-0.27	-0.08	N_2-NNH	0.19	0.55	0.74
20	Ru_2HfPb	-1.11	-0.48	-0.18	N_2-NNH	0.30	0.33	0.81
21	Ru_2HfSn	-1.01	-0.31	-0.01	N_2-NNH	0.30	0.40	0.81
22	Ru_2HfZn	-1.03	-0.28	-0.16	NH-NH_2	0.23	0.53	0.86
23	Ru_2NbIn	-0.88	-0.39	-0.12	N_2-NNH	0.27	0.23	0.80
24	Ru_2NbZn	-0.88	-0.25	-0.15	NH-NH_2	0.34	0.28	0.75
25	Ru_2ScGa	-1.20	-0.46	-0.23	NH-NH_2	0.37	0.36	0.81
26	Ru_2ScPb	-1.41	-0.63	-0.32	NH-NH_2	0.45	0.33	0.64
27	Ru_2ScSn	-1.36	-0.53	-0.24	NH-NH_2	0.39	0.43	0.68
28	Ru_2TaIn	-0.92	-0.42	-0.21	N_2-NNH	0.21	0.29	0.89
29	Ru_2TaZn	-0.89	-0.29	-0.17	NH-NH_2	0.24	0.36	0.73
30	Ru_2TiAl	-0.96	-0.27	-0.02	NH-NH_2	0.35	0.34	0.82
31	Ru_2TiPb	-1.02	-0.45	-0.08	N_2-NNH	0.37	0.20	0.57
32	Ru_2YAl	-0.93	-0.22	-0.12	NH-NH_2	0.19	0.53	0.80
33	Ru_2YGa	-1.02	-0.28	-0.15	NH-NH_2	0.39	0.35	0.67
34	Ru_2YPb	-1.25	-0.53	-0.19	NH-NH_2	0.47	0.26	0.54
35	Ru_2YSn	-1.20	-0.45	-0.11	NH-NH_2	0.44	0.31	0.53
36	Ru_2ZrGa	-1.02	-0.29	-0.09	NH-NH_2	0.22	0.51	0.79
37	Ru_2ZrIn	-1.15	-0.53	-0.35	NH-NH_2	0.33	0.29	0.66
38	Ru_2ZrPb	-1.05	-0.42	-0.09	N_2-NNH	0.34	0.29	0.76
39	Ru_2ZrTl	-1.09	-0.43	-0.21	NH-NH_2	0.35	0.31	0.61
40	Ru_2ZrZn	-1.09	-0.33	-0.24	NH-NH_2	0.40	0.36	0.84

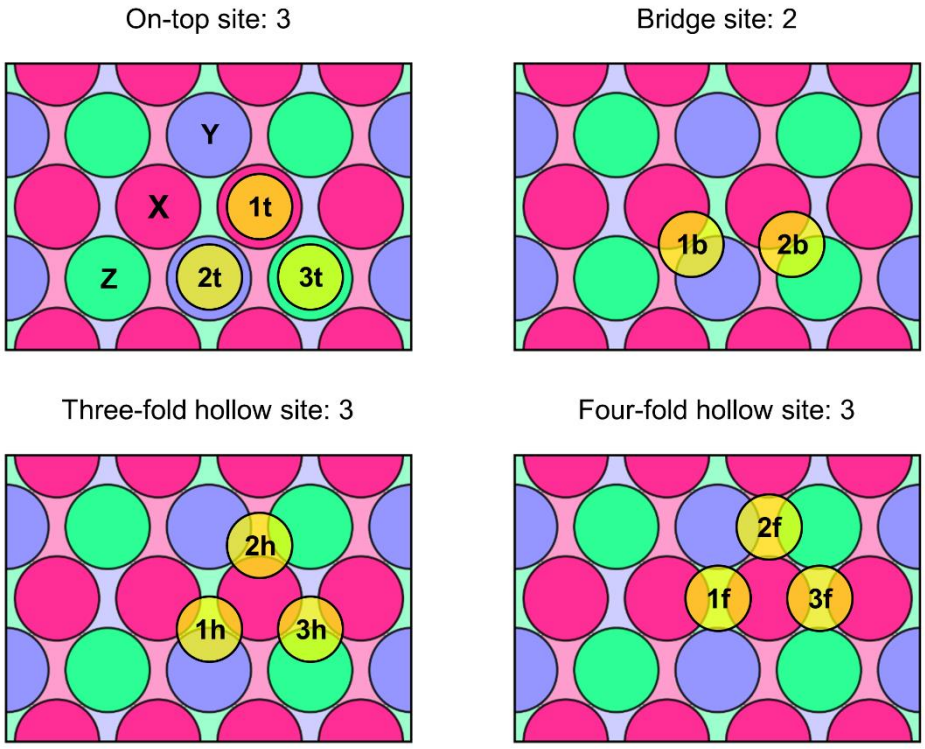

Supplementary Figure 1: Unique Adsorption Sites on (110) surface of Heusler alloy. "t", "b", "h" and "f" symbols represent on-top, bridge, three-fold hollow and four-fold hollow sites, respectively. Magenta, indigo, and green circles represent X, Y, and Z elements, respectively.

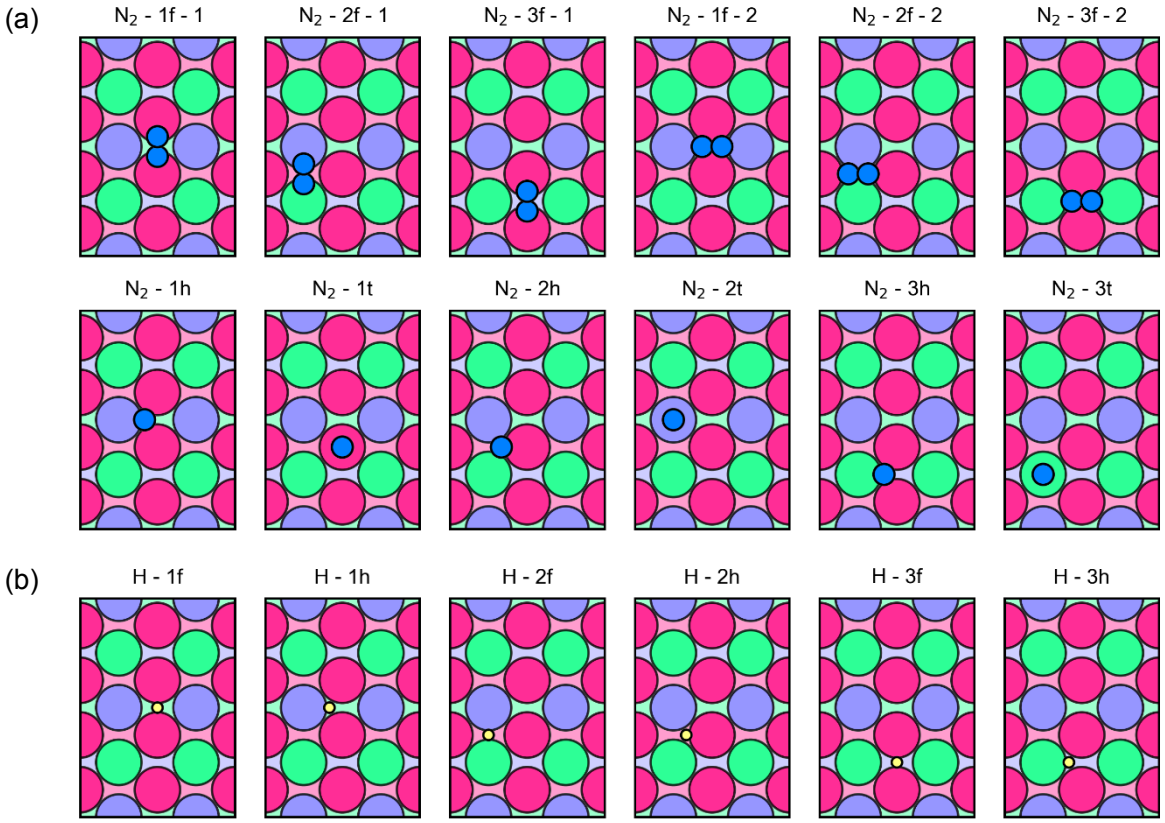

Supplementary Figure 2: Adsorption structures for (a) N_2 and (b) H. Magenta, indigo, green, blue, and yellow circles represent X, Y, Z, N, and H elements, respectively.

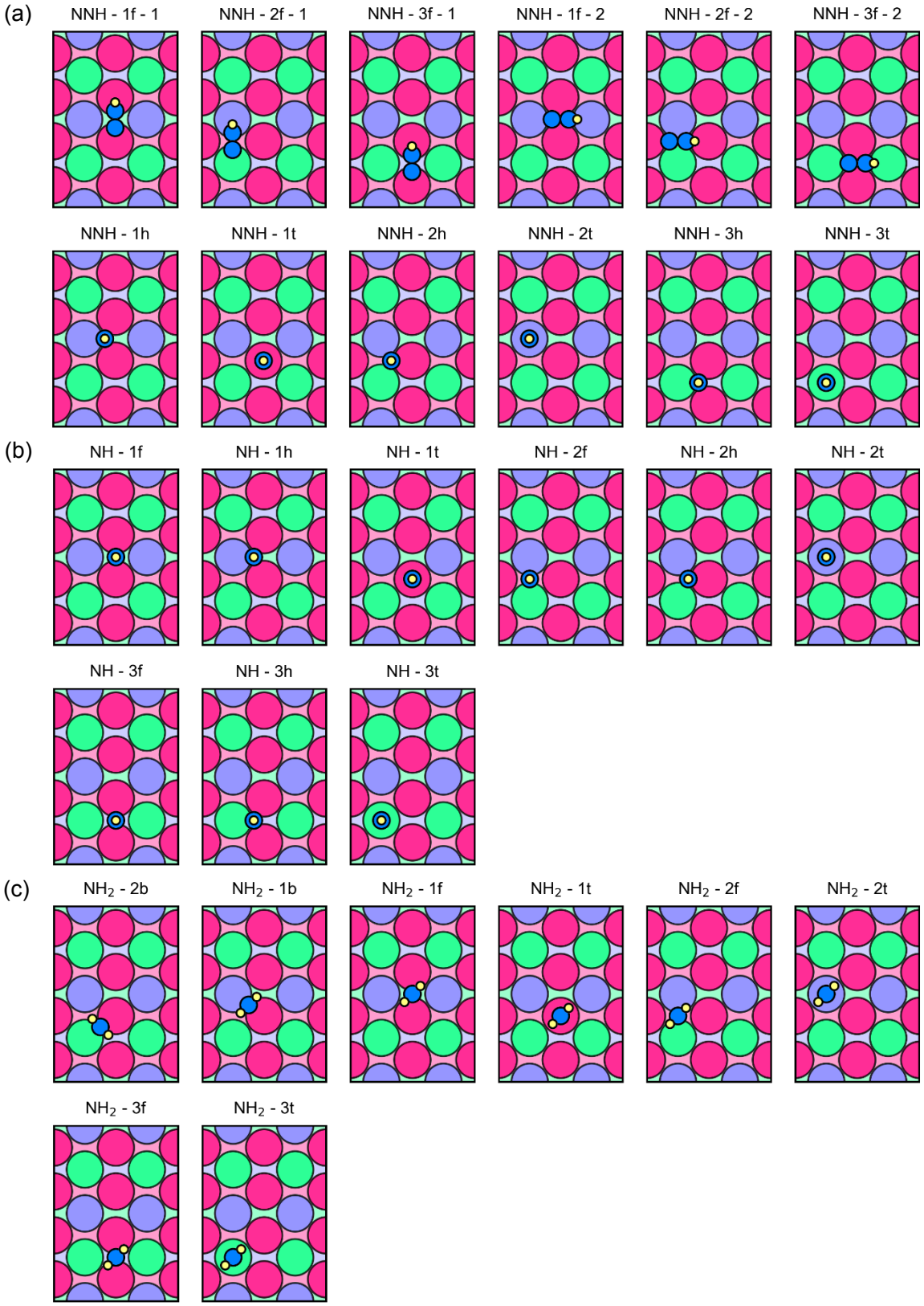

Supplementary Figure 3: Adsorption structures for (a) NNH, (b) NH and (c) NH_2. Magenta, indigo, green, blue, and yellow circles represent X, Y, Z, N, and H elements, respectively.

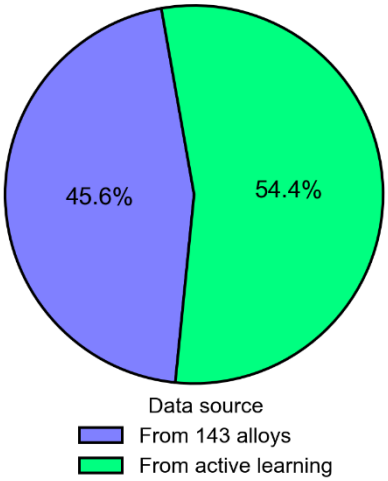

Supplementary Figure 4: The proportion of the data obtained from the initial 143 alloys and the data obtained by active learning sampling in the total data volume.

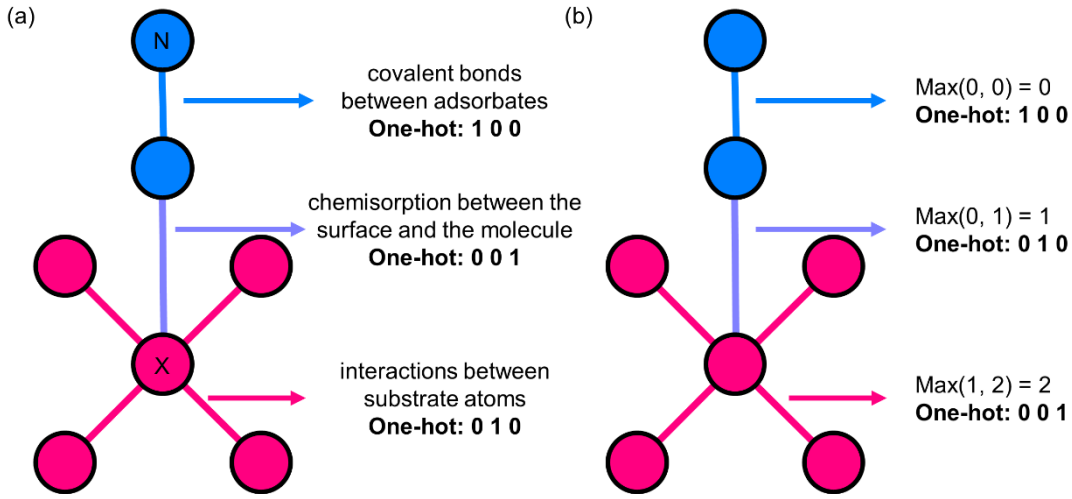

Supplementary Figure 5: Schematic representation of two edge features, (a) bond types, and (b) distance to the adsorbate. Magenta and blue circles represent X and N elements, respectively.

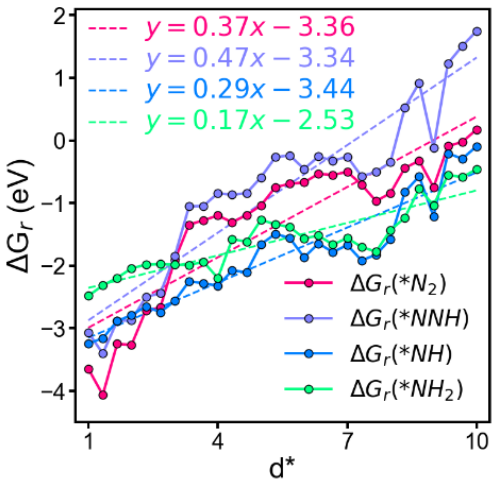

Supplementary Figure 6: $\Delta G_r(*N_2)$, $\Delta G_r(*NNH)$, $\Delta G_r(*NH)$ and $\Delta G_r(*NH_2)$ values as a function of d*.

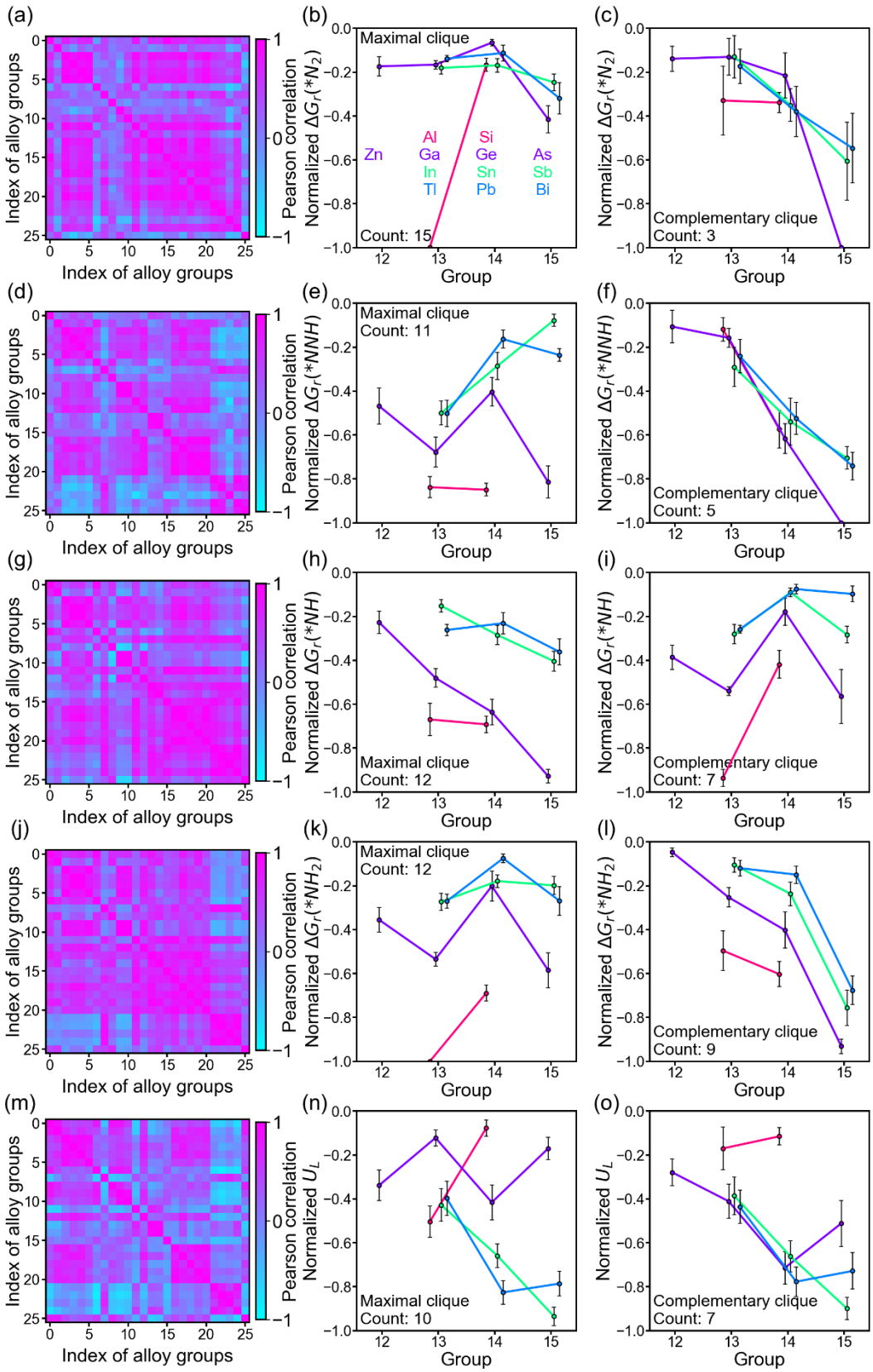

Supplementary Figure 7: (a), (d), (g), (j) and (m) are PCCs of ΔG_r and U_L changing trends with Z elements between each alloy group. (b), (e), (h), (k) and (n) are normalized average ΔG_r and U_L for alloy groups that within the maximal cliques, with the bars of the standard error of the mean. (c), (f), (i), (l) and (o) are normalized average ΔG_r and U_L for alloy groups within the complementary clique with the bars of the standard error of the mean.

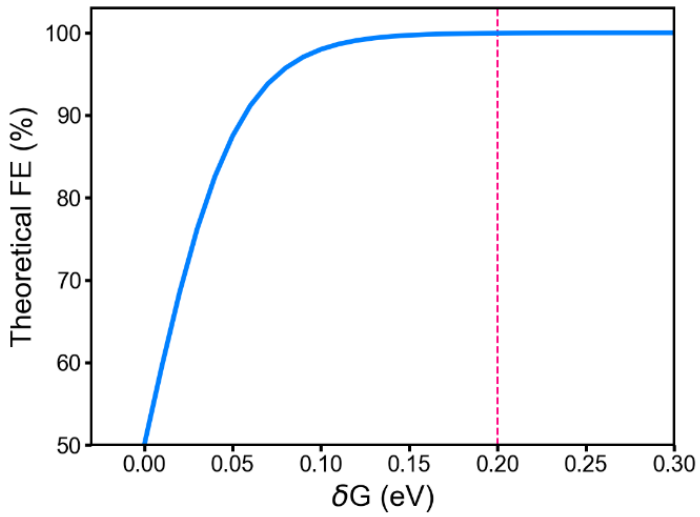

Supplementary Figure 8: The theoretical FE. It is calculated by $FE_{NRR}=\frac{1}{1+e^{-\frac{\delta G}{k_B T}}}\times 100\%$, where δG is Gibbs free energy difference between limiting potentials of HER and NRR, k_B is the Boltzmann constant, and T is the room temperature. The Magenta line is the threshold we set.

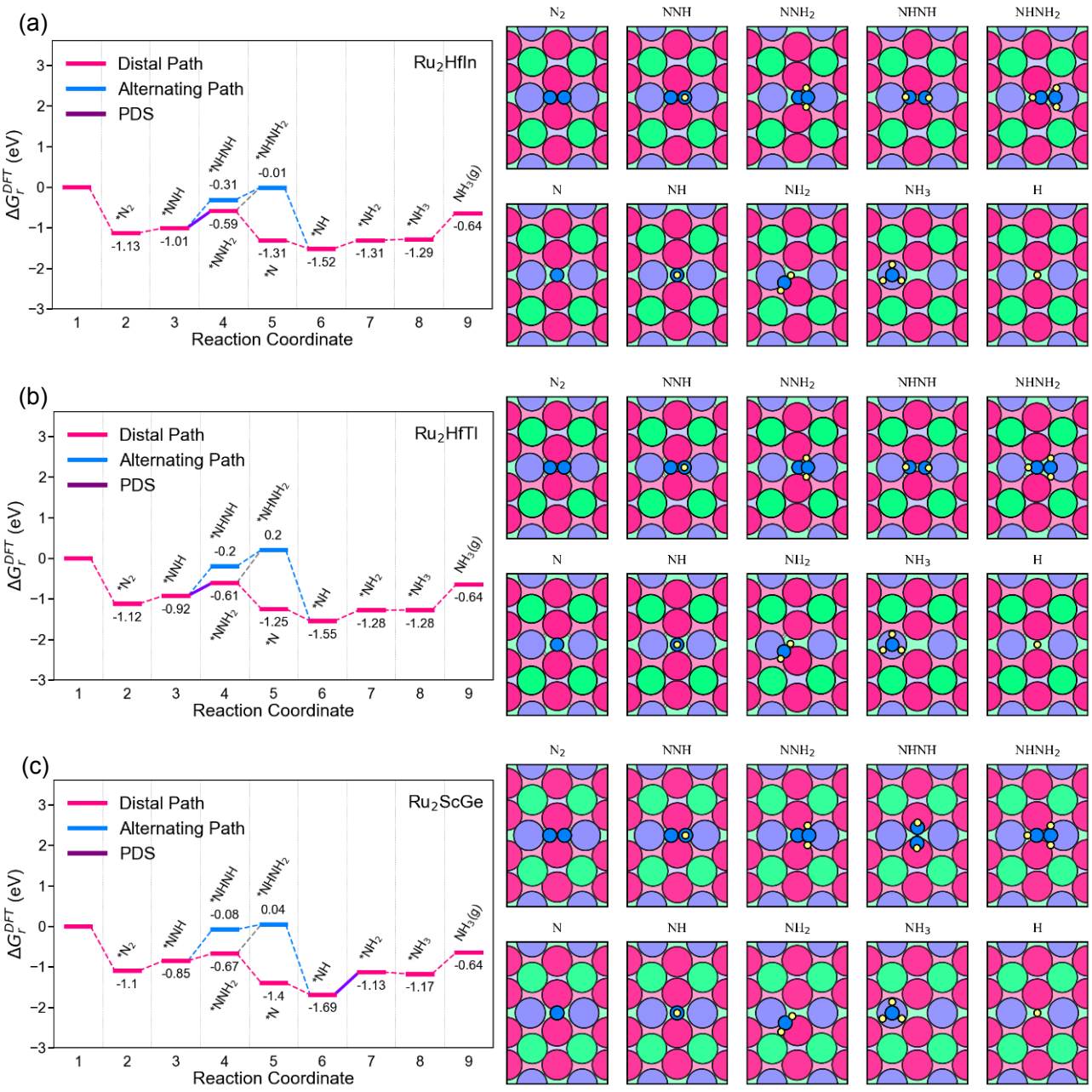

Supplementary Figure 9: (a), (b) and (c) are free energy diagrams and adsorption structures of individual intermediate on Ru_2HfIn, Ru_2HfTl and Ru_2ScGe, respectively. Grep lines represents mixed path. Magenta, indigo, green, blue, and yellow circles represent X, Y, Z, N, and H elements, respectively.

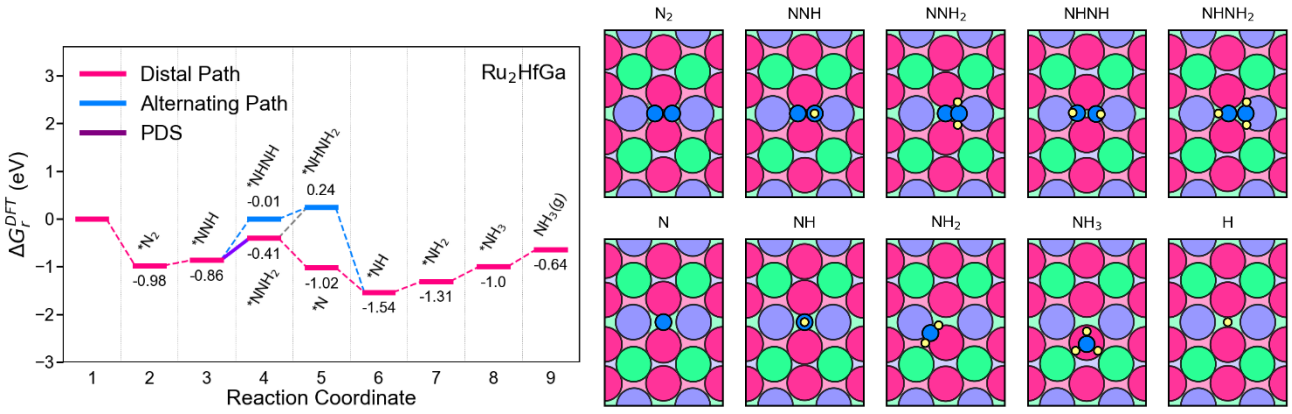

Supplementary Figure 10: Free energy diagram and adsorption structure on Ru_2HfGa. Grep lines represents mixed path. Magenta, indigo, green, blue and, yellow circles represent X, Y, Z, N, and H elements, respectively.

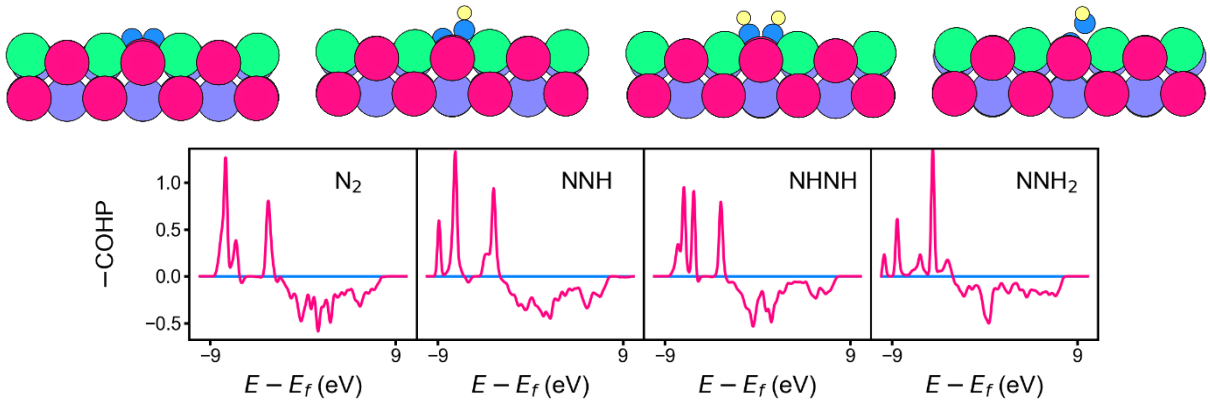

Supplementary Figure 11: Adsorption structures and COHPs for N_2, NNH, NHNH and NNH_2 adsorbed on Ru_2HfIn. Magenta, indigo, green, blue and yellow circles represent X, Y, Z, N and H elements, respectively. These COHPs are the average of all combinations between 2 N atoms and 2 Ru atoms.

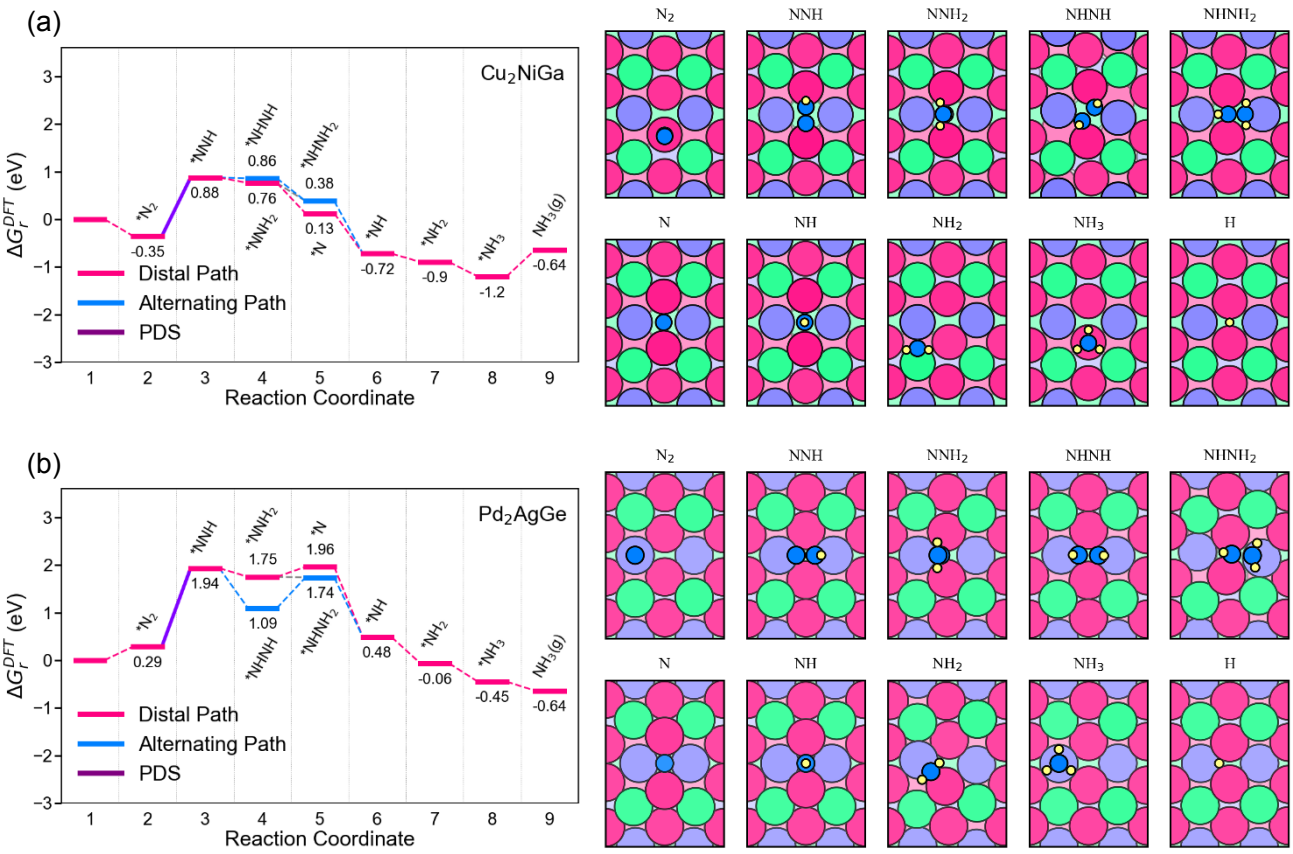

Supplementary Figure 12: Free energy diagrams and adsorption structures on Cu_2NiGa and Pd_2AgGe. Grep lines represents mixed path. Magenta, indigo, green, blue, and yellow circles represent X, Y, Z, N, and H elements, respectively.

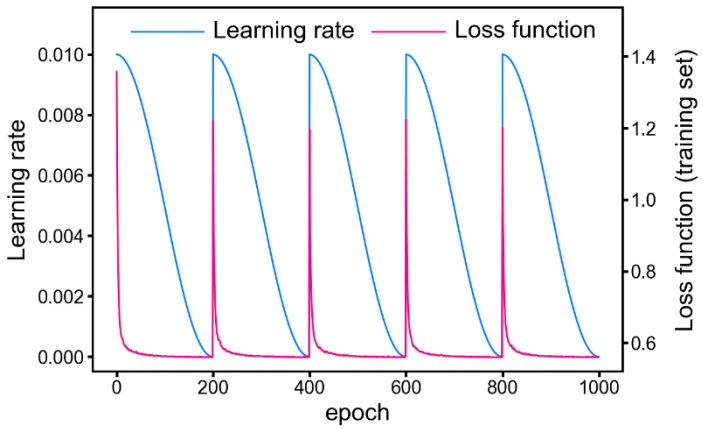

Supplementary Figure 13: Changes in the learning rate and loss function in the training set when using the snapshot ensembling method to train the final ASGCNN.